μ-Conotoxin GIIIA Interactions with the Voltage-Gated Na^+ Channel Predict a Clockwise Arrangement of the Domains

Samuel C. Dudley Jr.,*‡§ Nancy Chang,‖ Jon Hall,* Gregory Lipkind,¶** Harry A. Fozzard,¶ and Robert J. French‡‡

From the *Department of Medicine, ‡Department of Physiology, Emory University, Atlanta, Georgia 30322; §Atlanta Veterans Administration Medical Center, Atlanta, Georgia 30033; ‖Department of Anesthesiology, Brigham and Woman's Hospital, Boston, Massachusetts 02115; ¶Department of Neurobiology, Pharmacology and Physiology, **Department of Biochemistry and Molecular Biology, University of Chicago, Chicago, Illinois 60637; and ‡‡Department of Physiology and Biophysics, University of Calgary, Calgary, Alberta, Canada T2N 4N1

ABSTRACT Voltage-gated Na^+ channels underlie the electrical activity of most excitable cells, and these channels are the targets of many antiarrhythmic, anticonvulsant, and local anesthetic drugs. The channel pore is formed by a single polypeptide chain, containing four different, but homologous domains that are thought to arrange themselves circumferentially to form the ion permeation pathway. Although several structural models have been proposed, there has been no agreement concerning whether the four domains are arranged in a clockwise or a counterclockwise pattern around the pore, which is a fundamental question about the tertiary structure of the channel. We have probed the local architecture of the rat adult skeletal muscle Na^+ channel (μ1) outer vestibule and selectivity filter using μ-conotoxin GIIIA (μ-CTX), a neurotoxin of known structure that binds in this region. Interactions between the pore-forming loops from three different domains and four toxin residues were distinguished by mutant cycle analysis. Three of these residues, Gln-14, Hydroxyproline-17 (Hyp-17), and Lys-16 are arranged approximately at right angles to each other in a plane above the critical Arg-13 that binds directly in the ion permeation pathway. Interaction points were identified between Hyp-17 and channel residue Met-1240 of domain III and between Lys-16 and Glu-403 of domain I and Asp-1532 of domain IV. These interactions were estimated to contribute -1.0 ± 0.1, -0.9 ± 0.3, and -1.4 ± 0.1 kcal/mol of coupling energy to the native toxin–channel complex, respectively. μ-CTX residues Gln-14 and Arg-1, both on the same side of the toxin molecule, interacted with Thr-759 of domain II. Three analytical approaches to the pattern of interactions predict that the channel domains most probably are arranged in a clockwise configuration around the pore as viewed from the extracellular surface.

KEY WORDS: electrophysiology • site-directed mutagenesis • molecular models • kinetics • binding sites

INTRODUCTION

Knowledge of the structure of the voltage-gated Na^+ channel is necessary to understand its various functions and to optimize the pharmacokinetics of antiarrhythmic, local anesthetic, and anticonvulsant drugs. Although the K^+ channel pore-forming tetramer complex has been successfully analyzed by diffraction techniques (Doyle et al., 1998), the Na^+ channel has been resistant so far to such analysis. The Na^+ channel consists of four homologous domains of a single polypeptide arranged circumferentially around a central ion permeation pathway. These similar, but nonidentical, domains could be organized either in a clockwise or in a counterclockwise pattern around the central pore. No experimental data are available to distinguish between these alternative patterns. Molecular models of the channel have been divided on this point: four proposing a clockwise arrangement (Lipkind and Fozzard, 1994; Pérez-García et al., 1996; Schlief et al., 1996; Bénitah et al., 1997), and four proposing a counterclockwise arrangement (Guy, 1988; Schild and Moczydlowski, 1994; Chiamvimonvat et al., 1996; Pérez-García et al., 1997).

μ-Conotoxin GIIIA (μ-CTX)[1] is a 22–amino acid peptide toxin, originally isolated from piscivorous cone snails, that binds Na^+ channels (Olivera et al., 1990). Three disulfide bonds confer structural rigidity on the toxin, and its solution structure has been solved by nuclear magnetic resonance (Lancelin et al., 1991; Ott et al., 1991; Wakamatsu et al., 1992). The μ-CTX binding

Address correspondence to Samuel C. Dudley Jr., MD, Ph.D., Assistant Professor of Medicine and Physiology, Division of Cardiology, Emory University/VAMC, 1670 Clairmont Road, Room 111B, Decatur, GA 30033. Fax: (404) 329-2211; E-mail: sdudley@emory.edu

[1]*Abbreviations used in this paper:* ΔG, the change in free energy of binding; ΔΔG, interaction energy; Hyp, hydroxyproline; IC_{50}, 50% inhibitory concentration; k_{off}, off rate; k_{on}, on rate; μ-CTX, μ-conotoxin GIIIA; μI, rat adult skeletal muscle Na^+ channel; neoSTX, neosaxitoxin; STX, saxitoxin; τ_{off}, exponential time constant for relief of toxin block; τ_{on}, exponential time constant for toxin block; TTX, tetrodotoxin.

site overlaps that of tetrodotoxin (TTX) and saxitoxin (STX; Moczydlowski et al., 1986; Stephan et al., 1994; Chahine et al., 1995; Dudley et al., 1995; Li et al., 1997; Chang et al., 1998), but it is not identical to it. The blocking mechanism of these site 1 toxins appears to be binding to the outer vestibule and occlusion of the pore by a guanidinium group (Kao, 1986; Sato et al., 1991; Becker et al., 1992; Chahine et al., 1995; French et al., 1996; Chang et al., 1998; Todt et al., 1999).

Previously, we have shown interactions of the critical guanidinium group on Arg-13 of μ-CTX with predominantly two acidic residues of the adult rat skeletal muscle Na^+ channel (μI) outer vestibule, Glu-403 and Glu-758 (Chang et al., 1998). These two residues are thought to be within the outer vestibule, but located extracellular to the selectivity filter (Terlau et al., 1991; Chiamvimonvat et al., 1996; Yamagishi et al., 1997). Directly above Arg-13 of μ-CTX is a group of four residues (Asp-12, Gln-14, Hyp-17, and Lys-16) arranged in a plane and at approximately right angles to each other, forming a collar around Arg-13 (DQHypK collar; Fig. 1). Three of these residues are known to have significant effects on μ-CTX binding (Sato et al., 1991; Becker et al., 1992; Chahine et al., 1995). We suggested that the DQHypK collar interacted with the outer vestibule to prevent Arg-13 of μ-CTX from more closely approaching the selectivity filter (Chang et al., 1998). In a molecular model explaining the observed channel interactions with μ-CTX Arg-13, the Na^+ channel domains were arranged in a clockwise manner around the central axis of the pore as viewed from the extracellular surface; the DQHypK collar tetrad was oriented such that Asp-12, Gln-14, Hyp-17, and Lys-16 were approximating domains I, II, III, and IV, respectively.

Specific channel–toxin interactions can be inferred by mutant cycle analysis (Horovitz et al., 1990; Serrano et al., 1990; Fersht et al., 1992). With this approach, the interdependence of the effects on the toxin blocking

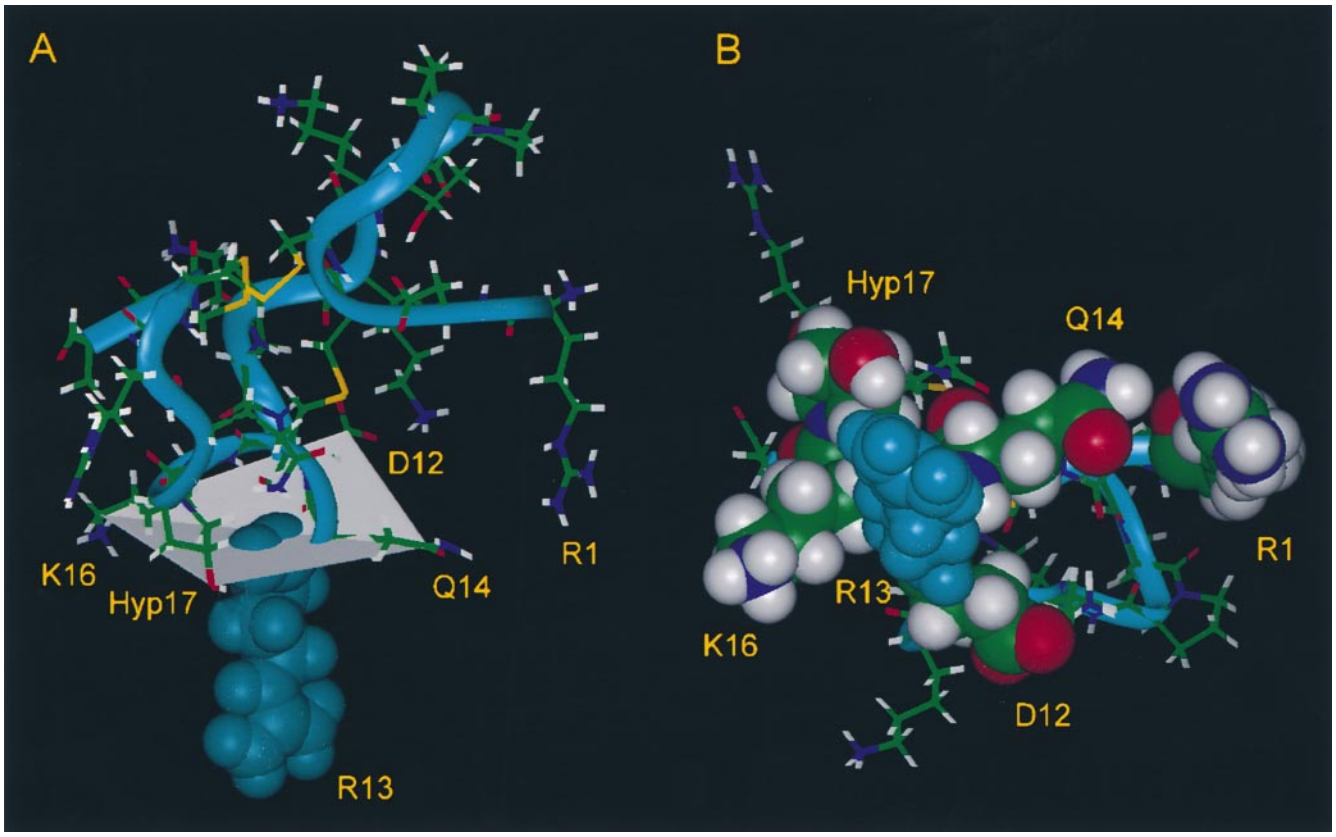

FIGURE 1. μ-Conotoxin GIIIA as a structural template for the Na^+ channel vestibule. The backbone structure is taken from the Protein Data Bank (.pdb) file for the mean structure determined from NMR data. The free amino acid side chains were oriented in the extended conformation, and the toxin was subjected to energy minimization. Based upon the coupling data, the position of the Arg-1 side chain was adjusted toward the Arg-13 end of the toxin. (A) The collar tetrad of μ-CTX defined by Asp-12, Gln-14, Hyp-17, and Lys-16 (DQHypK) as viewed from the side. The critical Arg-13, which is required for current block, is directed downward and is shown in light blue CPK format. The four collar tetrad amino acids are arranged with side chains oriented at roughly right angles to each other in a plane above Arg-13, and three of the four have been shown to be important for μ-CTX binding. (B) The collar tetrad of μ-CTX as viewed from below the toxin (i.e., from the intracellular side when the toxin is docked in the pore). The critical Arg-13 (light blue) is directed toward the viewer. The collar tetrad amino acids and Arg-1 are shown in CPK format. This view demonstrates that Arg-1 is on the same side of the toxin as Gln-14. Carbon, nitrogen, oxygen, sulfur, and hydrogen are green, blue, red, yellow, and white, respectively.

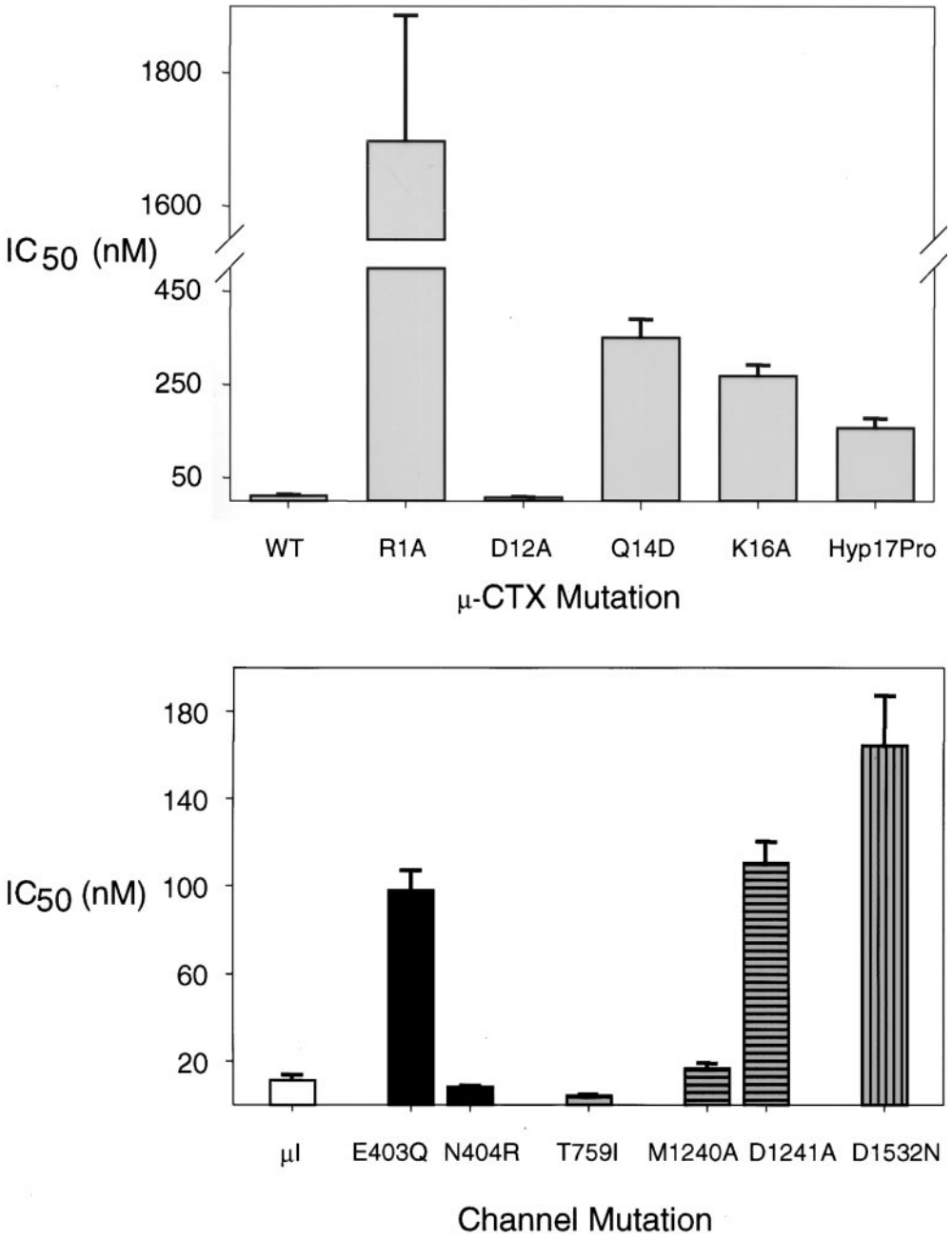

FIGURE 2. (Top) IC_{50}s of μ-CTX mutants for wild-type μI. The toxin R1A mutation resulted in the largest decrease in toxin blocking efficacy, 152-fold. Mutations in three of the four residues in the collar tetrad significantly reduced toxin affinity, suggesting that they have significant interactions with the channel. (Bottom) Native μ-CTX IC_{50}s for wild-type and mutant channels. Outer vestibule channel mutations in each of the domains were chosen because of interactions with the collar tetrad predicted by a molecular model of toxin binding (Chang et al., 1998). Two mutations were made in domains I (E403Q and N404R) and III (M1240A and D1241A). Within these domains, the effect of mutations is highly selective. E403Q and D1241A show significant reductions in native toxin affinity, but mutations of their adjacent residues, N404R and M1240A, cause little alteration in toxin IC_{50}. A single mutation in each of domains II (T759I) and IV (D1532N) was evaluated. D1532N results in the largest reduction in the native toxin IC_{50} of any of these outer vestibule mutations, a 15-fold change. The native μ-CTX IC_{50} for the wild-type channel is repeated from the top. Channel domains I, II, III, and IV are indicated by bars filled with black, gray, horizontal stripes, and vertical stripes, respectively.

efficacy of toxin and channel mutations is taken as evidence of an interaction. The degree of interdependence can be used to calculate a coupling energy between the reactive groups (Schreiber and Fersht, 1995). In this study, we tested our previous hypotheses about the interactions of the collar tetrad with outer vestibule amino acids from each of the four channel domains using mutant cycle analysis.

MATERIALS AND METHODS

The methods are similar to those previously used and have been described in detail (Chang et al., 1998). Native μ-CTX was synthesized as detailed below or obtained from either RBI or Sigma-Aldrich. μ-CTX from all three sources was equivalent in blocking activity.

μ-CTX Mutations

μ-CTX mutations were made by solid phase synthesis using 9-fluorenylmethoxycarbonyl (Fmoc) chemistry (Becker et al., 1989, 1990; Chang et al., 1998). The syntheses were performed on a polystyrene-based Rink amide resin that delivered the required amidated toxin upon cleavage. The peptides were air oxidized and HPLC purified, showing a single major peak on the chromatogram. Peptide composition was verified by quantitative amino acid analysis, supplemented as necessary with molecular weight determinations by mass spectroscopy for some derivatives. In three cases (Q14D, K16A, and Hyp17P), one dimensional proton nuclear magnetic resonance spectra for the toxin mutants

Table I

IC_{50} Values for Interactions between μ-CTX Derivatives and Different Na^+ Channel Mutants

	μI	E403Q	N404R	T759I	M1240A	D1241A	D1532N
	nM	*nM*	*nM*	*nM*	*nM*	*nM*	*nM*
μ-CTX	11 ± 3 (16)*	98 ± 9 (7)‡	8 ± 1 (5)	4 ± 1 (6)	17 ± 2 (9)	111 ± 10 (10)	164 ± 23 (15)‡
D12	7 ± 2 (10)	74 ± 13 (6)	12 ± 2 (7)	1 ± 1 (3)	9 ± 3 (4)	ND	ND
Q14D	351 ± 39 (9)	2,344 ± 269 (3)	415 ± 120 (3)	589 ± 80 (6)	ND	ND	4,269 ± 630 (6)
K16A	267 ± 24 (6)	576 ± 22 (5)	140 ± 22 (4)	348 ± 33 (5)	673 ± 97 (4)	ND	438 ± 44 (7)
Hyp17P	157 ± 21 (7)	895 ± 68 (5)	93 ± 12 (5)	87 ± 9 (3)	55 ± 8 (6)	2,722 ± 268 (8)	1,765 ± 293 (4)
R1A	1,697 ± 189 (8)	ND	ND	120 ± 12 (5)	ND	ND	ND

*15/16 experiments were previously reported by Chang et al., 1998. ‡Results were previously reported in Chang et al., 1998. ND, not determined.

were compared with published data for native μ-CTX. No evidence of improper folding was found. A complete structure has been reported for R13A, revealing no significant change in backbone arrangement when this critical residue is substituted (Wakamatsu et al., 1992), which is consistent with our own partial analyses. The synthetic technique yielded peptides that were ≥95% pure, as determined by analytical HPLC. The total peptide content of the samples was determined by quantitative amino acid analysis. Variance in weighing was estimated to lead to no more than a 10% error in calculating the toxin concentration.

Reagents were obtained from the following sources: Fmoc amino acids from Calbiochem-Novabiochem, Bachem, Genzyme, and Richelieu Biotechnologies; Rink amide resin was from Calbiochem-Novabiochem; and the coupling reagents were from Richelieu and Sigma-Aldrich.

Na^+ Channel Mutagenesis

Oligonucleotide-directed point mutations were introduced into the rat adult skeletal muscle Na^+ channel cDNA. DNA sequencing of the entire polymerized regions insured that only the intended mutations were present. Stage V and VI *Xenopus* oocytes from female frogs (NASCO or *Xenopus* 1) were injected with ~50–100 ng of cRNA. Oocytes were incubated at 16 for 12–72 h before examination.

Electrophysiology

Recordings were made by two-electrode voltage clamp at room temperature (20–22°C). The oocytes were placed in a bath chamber with a solution exchange time sufficiently short to resolve toxin blocking kinetics. The standard bath solution consisted of the following (in mM): 90 NaCl, 2.5 KCl, 1 $CaCl_2$, 1 $MgCl_2$, and 5 HEPES, titrated to pH 7.2 with 1 N NaOH. Recordings of the peak currents were made every 20 s upon step pulses from −100 to 0 mV. Only oocytes with between 1 and 10 μA of peak current were studied. The change in peak I_{Na} with time was fitted by single exponential functions and was used to estimate kinetic rate constants. The 50% inhibitory concentration (IC_{50}) for toxin binding was calculated from the ratio of peak currents in the absence and presence of toxin (Cruz et al., 1985; Moczydlowski et al., 1986). As previously described (Chang et al., 1998), agreement between the kinetic K_d and the equilibrium IC_{50}s was used to validate the measurements and was taken as evidence that toxin binding resulted in complete block for all mutations tested.

The free energy change in toxin binding to a wild-type/mutant channel pair (ΔG) was calculated as the difference of the average $RT\ln(IC_{50})$ for the wild-type and mutant, where R is the gas constant and T is temperature. The standard errors (SEMs) for ΔG were estimated as the square of the variance of the $RT\ln(IC_{50})$ averages divided by the square root of the sum of the

TABLE II

ΔΔG Values for Interactions between μ-CTX Derivatives and Different Na^+ Channel Mutants

	E403Q	N40R	T759I	M1240A	D1241A	D1532N
	kcal/mol	*kcal/mol*	*kcal/mol*	*kcal/mol*	*kcal/mol*	*kcal/mol*
D12A	0.14 ± 0.12 (35)*	0.54 ± 0.12 (34)	−0.29 ± 0.17 (31)	−0.12 ± 0.14 (35)	ND	ND
Q14D	−0.29 ± 0.09 (31)	0.09 ± 0.11 (29)	0.83 ± 0.12 (33)	ND	ND	−0.21 ± 0.09 (42)
K16A	−0.96 ± 0.08 (30)	−0.36 ± 0.09 (27)	0.69 ± 0.12 (29)	0.17 ± 0.09 (31)	ND	−1.39 ± 0.09 (41)
Hyp17P	−0.37 ± 0.09 (31)	−0.26 ± 0.10 (30)	0.22 ± 0.13 (29)	−0.97 ± 0.10 (35)	0.20 ± 0.09 (37)	−0.24 ± 0.10 (39)
R1A	ND	ND	−1.00 ± 0.12 (31)	ND	ND	ND

*Degrees of freedom (n − 4). ND, not determined

number of observations. ΔΔG was taken as the difference of the ΔGs for μ-CTX and the toxin mutant ($\Delta\Delta G = (G_{WT,native} - G_{mutant,native}) - (G_{WT,mutant} - G_{mutant,mutant})$, where the first and second subscript positions refer to the channel and the toxin, respectively, and the standard error of this number was reported as the square root of the sum of the variances of the $RT\ln(IC_{50})$ averages (Bevington, 1969) divided by the square root of the number of degrees of freedom. Note that ΔΔG may be positive or negative, both representing a coupling interaction. The negative values represent less coupling energy between the mutant pair as compared with the native residue pair. A positive ΔΔG indicates that the introduced pair has more coupling energy after mutation relative to the native pair. This might occur as a result of relief of a preexisting repulsion or by the creation of a novel attraction between the new pair. Data are presented as means ± SEM. Statistical comparisons of ΔGs and ΔΔGs were performed using two-tailed *t* tests assuming unequal variances (Excel 97; Microsoft Corp.).

RESULTS

Our experimental goal was twofold: (1) to expand our understanding of the binding interactions of μ-CTX, and (2) to draw structural inferences about the channel by determining points of interaction between the DQHypK collar amino acids directly above the critical Arg-13 residue (Fig 1).

The Effect of Mutations on Toxin Blocking Efficacy

Fig. 2 (top) shows toxin blocking efficacy of the μ-CTX derivatives with the wild-type channel. The native μ-CTX affinity for the wild-type μI Na^+ channel was in the range of values reported by others for the rat skeletal muscle channel (Moczydlowski et al., 1986; Becker et al., 1992; Chen et al., 1992; Stephan et al., 1994; Chahine et al., 1995, 1998; Dudley et al., 1995; Li et al., 1997; Chang et al., 1998). All mutants other than D12A resulted in a significant decrease in toxin IC_{50}.

The effects of channel mutations from each of the four domain pore-forming loops on native μ-CTX affinity are shown in Fig. 2 (bottom). The choice of channel residues mutated was based upon previously predicted collar–channel interactions (Chang et al. 1998). Inspection of the macroscopic current kinetics and current–voltage curves showed no significant alteration in kinetics or reversal potential with any of the channel mutations. Of the two domain I mutations, Glu-403 appeared to be moderately important for native μ-CTX blocking, and Asn-404 appeared not to be important in determining the toxin equilibrium IC_{50}. N404R resulted in a modest increase in μ-CTX blocking efficacy, but this change was not statistically significant ($P = 0.28$). Since almost the entire loss of binding energy when mutating Arg-13 could be explained by the loss of the Arg-13/Glu-758 interaction (Chang et al., 1998), Glu-758 was not evaluated for other interactions in the present study. Isoleucine was introduced in place of Thr-759. This channel mutation resulted in modest increase in native μ-CTX blocking efficacy ($P = 0.02$). This is the first report of change in μ-CTX affinity with mutations at this channel site, and the modest change in toxin IC_{50} suggests little alteration in the outer vestibule by this channel mutant. The effects of channel mutations in domain III were highly selective. The IC_{50} of native μ-CTX for M1240A was not statistically different from the wild-type channel ($P = 0.1$). D1241A reduced μ-CTX IC_{50} by 10-fold. Of the channel residues tested in our experiments, domain IV Asp-1532 appeared to be the most important determinant of μ-CTX blocking efficacy. The size-conserving mutation, D1532N, resulted in a 15-fold reduction in the IC_{50} of the native toxin for the channel. Table I summarizes the effect of all combinations of toxin and channel mutants on IC_{50}.

Determination of Toxin–Channel Couplings

Mutant cycle analysis was used to determine coupling between μ-CTX and the outer vestibule. Results for all combinations of channel–toxin mutants tested are shown in Table II. The μ-CTX mutant Q14D showed a significant coupling to channel residue T759I (Fig. 3 A). Mutant cycles incorporating this toxin mutation showed a domain-specific pattern consistent with coupling between Gln-14 and the domain II residue Thr-759 (Fig. 3 B). The ΔΔG for the Q14D–T759I interaction relative to the native complex was statistically different ($P < 0.01$) from the ΔΔG values for the Q14D/N404R, Q14D/E403Q, and Q14D/D1532N.

Hyp-17 of μ-CTX showed a domain-specific interaction exclusively with Met-1240 of domain III (Fig. 3 B). This interaction is consistent with the Sδ of Met acting as a hydrogen bond receptor for the γ-OH of Hyp. The energy of this type of interaction has been shown to be ~1.1 kcal/mol (Wilkinson et al., 1983). The Hyp17P mutation resulted in a loss of toxin binding energy (ΔG) of ~1.5 kcal/mol. Therefore, most of this loss could be explained by elimination of the Hyp-17/Met-1240 interaction. The Hyp-17 interaction appeared specific for Met-1240 of domain III. No interaction was identified between the adjacent Asp-1241 and Hyp-17 ($\Delta\Delta G = 0.2 \pm 0.1$ kcal/mol), even though D1241A had a large effect on native μ-CTX affinity, and no other significant interactions were identified between Hyp-17 and channel residues of the other domains.

Lys-16 is opposite Gln-14 in the μ-CTX collar tetrad, and the K16A mutation resulted in the next largest reduction in blocking efficacy among the collar tetrad derivatives tested. As anticipated from the structure of μ-CTX and the interaction of Gln-14 with domain II, the toxin 16 site showed the strongest interaction with domain IV Asp-1532 (Fig. 3 B). However, the Lys-16 interaction was not confined to Asp-1532. An interaction of lesser energy was demonstrated with the domain I channel residue, Glu-403 ($P < 0.01$). Of less clear sig-

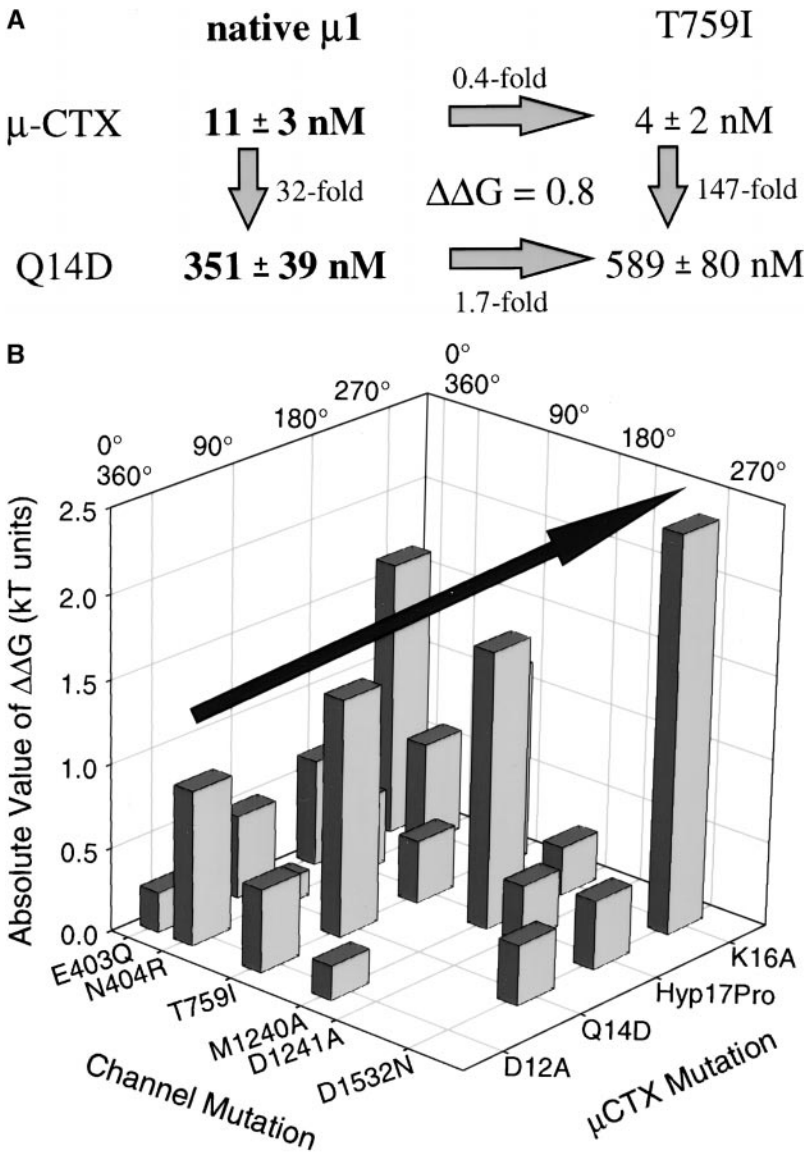

FIGURE 3. (A) A representative mutant cycle between Gln-14 of μ-CTX and Thr-759 of the channel. The presence of Ile in place of Thr at the channel 759 position influences the effect on toxin blocking efficacy seen with the Q14D mutation. This interdependence of the effects of the two mutations on the IC_{50} values suggests that the two residues interact. (B) The absolute values of interaction energies (in kT units) between toxin collar tetrad residues and various channel residues. Mutation of Asp-12 has little effect on toxin blocking efficacy, and mutant cycle analysis reveals no conclusive couplings between the toxin 12 site and the outer vestibule residues tested. Of the substitutions tested in the collar tetrad, μ-CTX mutant Q14D has the largest effect on toxin IC_{50} for the wild type μI channel. Coupling energies for this toxin mutation are domain-specific and suggest an interaction between the Gln-14 and domain II residue Thr-759. Of the channel residues tested, Hyp-17 of μ-CTX interacted exclusively with Met-1240 of domain III. The lack of coupling between Hyp-17 and the adjacent channel residue Asp-1241, which strongly influences toxin affinity, provides some evidence against the likelihood of confounding allosteric effects. μ-CTX Lys-16 shows the strongest interaction with domain IV Asp-1532, as expected based upon the position of Lys-16 in the collar tetrad of μ-CTX opposite that of Gln-14. Also, couplings of lesser energy with Glu-403 of domain I and Thr-759 of domain II are present. Channel residues from domains I, II, III, and IV are grouped. Angular positions represent nominal orientations defined by the domains and the collar tetrad residues. The arrow is intended to draw attention to the pattern of strong interactions when progressing around the collar tetrad residues.

nificance, an energetically opposite K16A–T759I interaction was observed that was statistically different from zero ($P < 0.01$).

No strong Asp-12 interactions were resolved by these experiments (Fig. 3 B). Because of the previously demonstrated interactions, the expectation was that Asp-12 would be adjacent to channel residues of domain I. The coupling with Asn-404 was small but statistically significant. Asp-12 showed no coupling with residues in domain II (Thr-759) or domain III (Met-1240).

The structure of the toxin (Lancelin et al., 1991; Wakamatsu et al., 1992) shows that μ-CTX Arg-1 and Gln-14 are both on the same side of the molecule. Therefore, we looked for possible interactions between Arg-1 and domain II. The toxin mutation R1A resulted in a 152-fold reduction in the toxin IC_{50} for the wild-type μI channel, confirming the importance of Arg-1 in μ-CTX binding. As predicted from the coupling between toxin residue Gln-14 and the domain II residue Thr-759, a significant interaction between Arg-1 and domain II was demonstrated. In summary, the coupling energy data identified most clearly the following pairs of interacting toxin–channel residues: Gln-14/Thr-759, Arg-1/Thr-759, Hyp-17/Met-1240, Lys-16/Asp-1532, and Lys-16/Glu-403.

DISCUSSION

In this study, interactions between four residues of μ-CTX and several residues in the rat skeletal muscle Na^+ channel outer vestibule were demonstrated by mutant cycle analysis. These interactions help define important elements for toxin–channel high affinity recognition and binding. Furthermore, the combination of the structure of μ-CTX and these demonstrated inter-

actions establish constraints on the domain organization of the Na^+ channel.

Consistency with Previous Results

For wild-type channels, the IC_{50}s of μ-CTX mutations D12A, Q14D, K16A, and Hyp17P were 0.6-, 31-, 24-, and 14-fold change, respectively, from the native toxin IC_{50}. These changes are consistent with previous reports. The slight increase in blocking efficacy seen with D12A is consistent with all other reports of the effect of neutralization of the negative charge at this site (Sato et al., 1991; Becker et al., 1992; Chahine et al., 1995). Similar to our 31-fold Q14D effect, Chahine et al. (1995) reported that the Q14E mutation decreased toxin blocking efficacy by 55-fold. The modest difference in these results may be caused by the larger size of the glutamic acid side chain compared with aspartic acid. The normalized increase in IC_{50} with the K16A was slightly larger than that of a previous report by Sato et al. (1991) using a rat diaphragm contraction bioassay. Nevertheless, the 24-fold change was similar to the ~21-fold change in the dissociation constant seen for K16Q in bilayers incorporating rat skeletal muscle Na^+ channels (Becker et al., 1992). The 14-fold increase in IC_{50} with Hyp17P mutations fell in the middle of the range noted previously for the elimination of the β-OH of Hyp (6–21-fold; Sato et al., 1991; Becker et al., 1992; Chahine et al., 1995). Finally, the effect of elimination of the charge at the Arg-1 site was larger than previous reports (Sato et al., 1991; Becker et al., 1992; Chahine et al., 1995). Differences in the assay method or differences in the amino acid substituted may explain the quantitative differences among the data.

The effects of channel mutants seen in this study were generally consistent with previous reports. The mutation E403Q increased the native μ-CTX IC_{50} by 8.9-fold, similar to a 4-fold increase reported previously for the identical mutation (Stephan et al., 1994). However, the reason for the discrepancy between these similar results and the lack of effect on μ-CTX binding by E403C (Li et al., 1997) is unclear. N404R resulted in a modest increase in μ-CTX blocking efficacy, and, under similar conditions, Chen et al. (1992) reported a slight increase in the IC_{50} (1.5-fold). Li et al. (1997) described mutations of Met-1240 and Asp-1241, substituting Cys, and came to the same conclusions about the effects of these two residues on μ-CTX blocking efficacy. Li et al. (1997) reported no effect on the IC_{50} with the D1532C mutation, in contrast to the large effect that we observed for the D1532N substitution. Moreover, Chiamvimonvat et al. (1996) and Tsushima et al. (1997) found that the mutation D1532C had a large effect on selectivity for NH_4^+ and K^+. Further studies are needed to identify the reason for these differences.

Interpretation of Interaction Energies

Toxins of known structure have proven extremely useful in probing the outer vestibule of K^+ channels (MacKinnon and Miller, 1989; MacKinnon et al., 1990, 1998; Park and Miller, 1992; Aiyar et al., 1995, 1996; Hidalgo and MacKinnon, 1995; Lu and MacKinnon, 1995; Gross and MacKinnon, 1996; Naranjo and Miller, 1996; Ranganathan et al., 1996; Swartz and MacKinnon, 1997). In principle, any individual amino acid may have multiple energetic interactions that contribute to the energy of binding. Mutant cycle analysis is a technique designed to isolate the coupling between a particular toxin–channel pair.

The major potential source of error with mutant cycle analysis arises from the possibility of structural changes in either of the interacting molecules as the direct result of mutations, or resulting secondarily from changes in the nature of the ligand–protein interaction. Allosteric effects can often be identified by generalized disruption of normal function of the channel. The mutated channels in this study were evaluated functionally, and they showed no significant alterations in the macroscopic gating behavior or reversal potential. Several toxin mutants have been screened for major structural changes by nuclear magnetic resonance with negative results. All toxin–channel pairs show blocking interactions, suggesting that the interacting surfaces were not grossly altered. Furthermore, the pattern of domain- and residue-specific ΔΔGs supported the specificity of interactions.

Of the interactions noted above, four showed negative ΔΔGs, and there was at least one positive ΔΔG. In performing mutant cycle analysis, mutations are usually chosen to eliminate interactions without inducing new ones. We defined the interaction energy such that negative energies of interaction would represent a loss of binding energy in the mutant pair complex compared with the native, bound complex. This idea is consistent with the negative ΔΔGs in the R1A/T759I, K16A/D1532N, K16A/E403Q, and Hyp17P/Met1240A pairs. Alternatively, a negative ΔΔG could arise from new repulsions resulting from the substituted residues as compared with the native ones. In either event, an interaction exists, implying that the residues are near enough to interact with each other in the toxin–channel complex. This dependence of ΔΔG on the choice of substituted residue was predicted by Faiman and Horovitz (1996).

The Q14D–T759I interaction showed a positive ΔΔG. Since the overall effect of the Q14D mutation was to decrease toxin blocking efficacy, the Gln-14/Thr-759 interaction is not sufficient to explain the entire Q14D effect. This could be the result of the double mutant complex eliminating a repulsion in the native complex or, less likely, adding a new attractive force between the toxin Asp and the channel Ile relative to the Gln/Thr

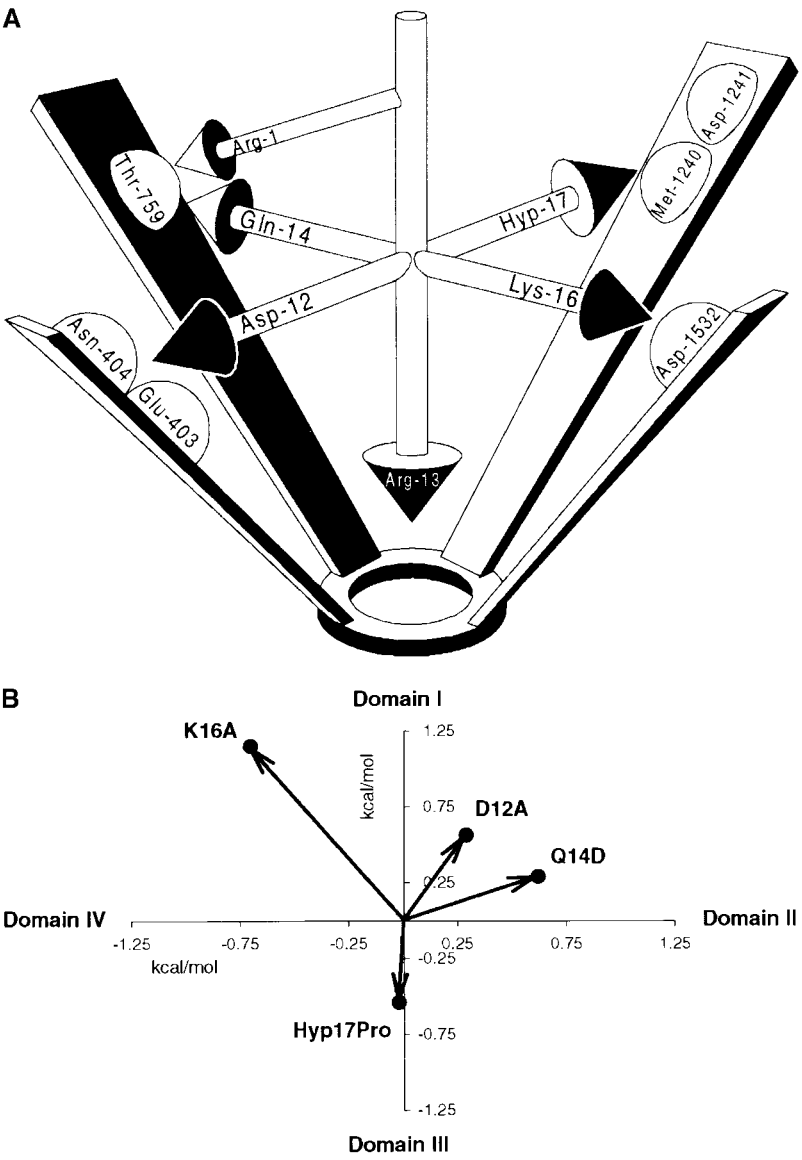

FIGURE 4. (A) An idealized, schematic representation of the orientations of the strongest interactions of μ-CTX with the channel. Arg-13 is oriented along the axis of permeation, and the DQ-HypK collar tetrad amino acids are shown in their orientation around Arg-13. The strongest ΔΔGs were shown between domains I, II, III, and IV and Asp-12, Gln-14, Hyp-17, and Lys-16, respectively. These interactions and the relationships of the collar tetrad amino acids to each other suggest that the channel domains are arranged in a clockwise manner as viewed from the extracellular surface around the axis of ion permeation. (B) Resultant interaction vectors (in kilocalories/mole) for collar tetrad residues are consistent with a clockwise arrangement of the channel domains as viewed from the extracellular surface. These interaction vectors empirically summarize the contributions of all 18 experimentally determined coupling energies. Channel domains are assumed to be arranged symmetrically around the pore axis in a clockwise, circumferentially sequential manner. For a given collar tetrad residue, the individual interaction vector is defined with the absolute value of an interaction energy as the amplitude, and a direction pointing toward the channel domain in question. Thus, interactions of a collar tetrad residue with domain I contribute positively on the ordinate, and domain III interactions contribute negatively. Similarly, domains II and IV interactions were counted as positive and negative along the abscissa, respectively. We note that the use of the absolute value of the interaction energy as the magnitude of the interaction vector is equivalent to the use by Hidalgo and MacKinnon (1995), Fig. 1, of coupling coefficients that are defined as being ≥1. For each collar tetrad residue, all of the individual interaction vectors were summed vectorially to create a resultant interaction vector that is plotted on the graph.

pair. The overall effect of T759I on native toxin binding is small, which is consistent with the opposing effects. It is plausible that there could be electrostatic repulsion between the substituted Asp-14 of the toxin and the negative residues of the vestibule, but Glu-403 and Asp-1532 must be too far away to contribute significantly. Consistent with this possibility, Li and his coworkers (Li, R.A., I.L. Ennis, S.C. Dudley Jr., R.J. French, G.F. Tomaselli, and E. Marban, manuscript submitted for publication) have noted significant interactions between Gln-14 and channel residues Asp-762 and Glu-765. This observation supports the conclusion that Gln-14 is oriented toward domain II.

The failure to show a Gln-14/Glu-403 interaction is consistent with the implication derived from the data of Stephan et al. (1994). In that study, the effects of E403Q on IC_{50}s for μ-CTX GIIIA and μ-CTX GIIIB IC_{50}s were determined. Among four amino acid differences with μ-CTX GIIIA, μ-CTX GIIIB contains a Q14R substitution. The ratio of the toxin IC_{50}s for wild-type and E403Q- mutated channels derived from these data were similar for μ-CTX GIIIA and μ-CTX GIIIB, suggesting that toxin site 14 and channel site 403 were not interacting significantly ($\Delta\Delta G = -0.3$ kcal/mol).

Our failure to demonstrate a strong interaction of Asp-12 with the channel does not preclude the possibility that Asp-12 is near domain I. In the Barstar–Barnase complex wherethe crystal structure could be determined, Schreiber and Fersht (1995) showed that there was a general relationship between the coupling energy and separation of the interaction partners, but that a lack of coupling could occur in closely approximated residues. Structural proximity alone was not sufficient to produce interactions. On the other hand, there was no coupling when the tested pair was separated by >8 Å. Therefore, they concluded that demonstration of

coupling set a distance limit on the separation of two residues. Perhaps, the charge of Asp-12 is neutralized in the native toxin by an intramolecular interaction with an adjacent toxin residue such as Lys-8, and therefore, elimination of charge at this residue has little effect on toxin–channel interactions. In any event, the absence of strong coupling is consistent with the lack of any significant influence of Asp-12 substitutions on toxin affinity.

The Lys-16 interaction pattern was more difficult to interpret. At a level considered to identify confidently interactions (Ranganathan et al., 1996), Lys-16 showed significant ΔΔGs with Asp-1532 of domain IV and Glu-403 of domain I, suggesting that Lys-16 might be located between these two domains. Multidomain interactions suggest that caution should be used when interpreting the effects of charge-changing mutations. In this case, the largest energy associated with the Lys-16/Asp-1532 interaction hints that Lys-16 might be closest to domain IV.

Because the M1240C mutation did not change the IC_{50} of native μ-CTX binding significantly, Backx and his coworkers (Li et al., 1997) concluded that Met-1240 played no role in toxin binding. Consistent with this assertion, our results demonstrated that the effect of M1240A on native μ-CTX blocking efficacy was small. On the other hand, a significant negative ΔΔG was calculated for the Hyp17Pro/M1240A interacting pair. This suggests that the net effect of Met-1240 mutations is the sum of at least two interactions with opposing energetic effects. Our study supports previous demonstrations that Asp-1241 is important for μ-CTX binding (Li et al., 1997), but the toxin residue interacting with Asp-1241 is not identified in either study.

Structural Implications of Coupling Data

Our experimentally derived coupling data are most consistent with a circumferentially sequential, clockwise arrangement of the domains around the ion permeation pathway. Gln-14, Hyp-17, and Lys-16 are arranged at approximately right angles to each other in a plane perpendicular to the axis of the pore. These toxin residues interact most strongly with residues of domains II, III, and IV, respectively. These interactions are best explained if the domains are arranged in the clockwise pattern, as shown in Fig. 4. In the structure of μ-CTX, Arg-1 is on the same side of the toxin as Gln-14, and its coupling with a domain II residue also supports the clockwise domain arrangement.

Three different approaches to the interpretation of our observations all lead to this conclusion. First, an intuitive approach in which the strongest coupling of each collar residue is considered to dominate and define the orientation in the pore indicates a clockwise arrangement as shown in Fig. 4 A. Second, to systematically take into account all of our coupling data, rather than make conclusions using selectively identified strong interactions, we devised a novel analysis based on defining a resultant interaction vector for each of the collar tetrad residues. Within the data set, this analysis provides an unbiased summary of statistically significant multidomain interactions, such as those of the charged residue Lys-16, which, when considered in isolation, would suggest couplings in several directions. Shown in Fig. 4 B (see figure legend for details), this analysis argues for a clockwise domain orientation. Determination of additional couplings may affect quantitatively the interaction vectors, but is unlikely to alter the basic clockwise conclusion. Finally, the common conclusion, a clockwise domain arrangement, is further supported by a statistical analysis of the collected interaction energy data. The sums of ΔΔGs for each of the eight possible sequential clockwise and counterclockwise configurations of the domain–collar interactions were made and the variances were calculated. The most favorable clockwise configuration was as shown in Fig. 4 A. This was tested against the two most favorable counterclockwise conformations. In both comparisons, the clockwise configuration was favored, with $P < 0.001$.

There are a limited number of toxin–channel interactions that can be elucidated with a single toxin, so it is important to test multiple toxins of differing shapes to constrain models adequately. A multiple toxin approach minimizes the possibility of being misled by allosteric changes produced by mutagenesis. The conclusions about channel architecture inferred here from μ-CTX–channel interactions are similar to those derived from STX–channel interactions (Penzotti, J.L., G.M. Lipkind, H.A. Fozzard, and S.C. Dudley Jr., manuscript submitted for publication). Interactions derived using neoSTX and μ-CTX, two toxins with significantly different structures and chemical interactions, support the validity of the general features of the model in Fig. 4 A, and set the stage for further tests of outer vestibule structural predictions.

Ian Glaaser, Colleen Parrett, Junxiu Ling, and Bin Xu provided technical assistance. The authors thank Dr. Jack Kyle and Dr. Steven Chang for their assistance, Dr. Denis McMaster for synthesizing peptides, Dr. D. McIntyre and P. Hwang for NMR data, Dr. Kwokyin Hui for testing some toxin derivatives by single channel recording, and Drs. R.A. Li, I.L. Ennis, G.F. Tomaselli, and E. Marban for sharing submitted manuscripts. We thank Dr. Richard Horn for helpful discussions.

This research was supported by an American Heart Association, Southeast Affiliate Beginning Grant-in-Aid (to S.C. Dudley), by a Program Project Award from the National Institutes of Health (to H.A. Fozzard, No. P01-HL20592), and by an operating grant from the Medical Research Council of Canada (to R.J. French). S.C. Dudley is supported by a Scientist Development Award from the American Heart Association, a Procter and Gamble University Research Exploratory Award, and National Institutes of Health Grant (HL64828). N.S. Chang was supported by the training grant TO1-GM07019. R.J. French received salary support as an Alberta

Heritage Foundation for Medical Research Medical Scientist and a Medical Research Council Distinguished Scientist.

Submitted: 4 April 2000
Revised: 13 September 2000
Accepted: 15 September 2000

REFERENCES

Aiyar, J., J.M. Withka, J.P. Rizzi, D.H. Singleton, G.C. Andrews, W. Lin, J. Boyd, D.C. Hanson, M. Simon, B. Dethlefs, C.L. Lee, J.E. Hall, G.A. Gutman, and K.G. Chandy. 1995. Topology of the pore-region of a K^+ channel revealed by the NMR-derived structures of scorpion toxins. *Neuron.* 15:1169–1181.

Aiyar, J., J.P. Rizzi, G.A. Gutman, and K.G. Chandy. 1996. The signature sequence of voltage-gated potassium channels projects into the external vestibule. *J. Biol. Chem.* 271:31013–31016.

Becker, S., E. Atherton, and R.D. Gordon. 1989. Synthesis and characterization of μ-conotoxin IIIa. *Eur. J. Biochem.* 185:79–84.

Becker, S., R. Liebe, and R.D. Gordon. 1990. Synthesis and characterization of an N-terminal-specific I-125-photoaffinity derivative of μ-conotoxin GIIIA which binds to the voltage-dependent sodium channel. *FEBS Lett.* 272:152–154.

Becker, S., E. Prusak-Sochaczewski, G. Zamponi, A.G. Beck-Sickinger, R.D. Gordon, and R.J. French. 1992. Action of derivatives of μ-conotoxin GIIIA on sodium channels. Single amino acid substitutions in the toxin separately affect association and dissociation rates. *Biochemistry.* 31:8229–8238.

Bénitah, J.P., R. Ranjan, T. Yamagishi, M. Janecki, G. Tomaselli, and E. Marban. 1997. Molecular motions within the pore of voltage-dependent sodium channels. *Biophys. J.* 73:603–613.

Bevington, P.R. 1969. Propagation of errors. *In* Data Reduction and Error Analysis for the Physical Sciences. P.R. Bevington, editor. McGraw-Hill Book Company, New York. 56–65.

Chahine, M., L.Q. Chen, N. Fotouhi, R. Walsky, D. Fry, V. Santarelli, R. Horn, and R.G. Kallen. 1995. Characterizing the μ-conotoxin binding site on voltage-sensitive sodium channels with toxin analogs and channel mutations. *Recept. Channels.* 3:161–174.

Chahine, M., J. Sirois, P. Marcotte, L. Chen, and R.G. Kallen. 1998. Extrapore residues of the S5-S6 loop of domain 2 of the voltage-gated skeletal muscle sodium channel (rSkM1) contribute to the μ-conotoxin GIIIA binding site. *Biophys. J.* 75:236–246.

Chang, N.S., R.J. French, G.M. Lipkind, H.A. Fozzard, and S.C. Dudley Jr. 1998. Predominant interactions between μ-conotoxin Arg-13 and the skeletal muscle Na^+ channel localized by mutant cycle analysis. *Biochemistry.* 37:4407–4419.

Chen, L.Q., M. Chahine, R.G. Kallen, R.L. Barchi, and R. Horn. 1992. Chimeric study of sodium channels from rat skeletal and cardiac muscle. *FEBS Lett.* 309:253–257.

Chiamvimonvat, N., M.T. Pérez-García, R. Ranjan, E. Marban, and G.F. Tomaselli. 1996. Depth asymmetries of the pore-lining segments of the Na^+ channel revealed by cysteine mutagenesis. *Neuron.* 16:1037–1047.

Cruz, L.J., W.R. Gray, B.M. Olivera, R.D. Zeikus, L. Kerr, D. Yoshikami, and E. Moczydlowski. 1985. *Conus geographus* toxins that discriminate between neuronal and muscle sodium channels. *J. Biol. Chem.* 260:9280–9288.

Doyle, D.A., J.M. Cabral, R.A. Pfuetzner, A. Kuo, J.M. Gulbis, S.L. Cohen, B.T. Chait, and R. MacKinnon. 1998. The structure of the potassium channel: molecular basis of K^+ conduction and selectivity. *Science.* 280:69–77.

Dudley, S.C., Jr., H. Todt, G. Lipkind, and H.A. Fozzard. 1995. A μ-conotoxin-insensitive Na^+ channel mutant: possible localization of a binding site at the outer vestibule. *Biophys. J.* 69:1657–1665.

Faiman, G.A., and A. Horovitz. 1996. On the choice of reference mutant states in the application of the double-mutant cycle method. *Protein Eng.* 9:315–316.

Fersht, A.R., A. Matouschek, and L. Serrano. 1992. I. Theory of protein engineering analysis of stability and pathway of protein folding. *J. Mol. Biol.* 224:771–782.

French, R.J., E. Prusak-Sochaczewski, G.W. Zamponi, S. Becker, A.S. Kularatna, and R. Horn. 1996. Interactions between a pore-blocking peptide and the voltage sensor of the sodium channel: an electrostatic approach to channel geometry. *Neuron.* 16:407–413.

Gross, A., and R. MacKinnon. 1996. Agitoxin footprinting the Shaker potassium channel pore. *Neuron.* 16:399–406.

Guy, H.R. 1988. A model relating the structure of the sodium channel to its function. *Curr. Top. Membr. Transp.* 33:289–308.

Hidalgo, P., and R. MacKinnon. 1995. Revealing the architecture of a K^+ channel pore through mutant cycles with a peptide inhibitor. *Science.* 268:307–310.

Horovitz, A., L. Serrano, B. Avron, M. Bycroft, and A.R. Fersht. 1990. Strength and co-operativity of contributions of surface salt bridges to protein stability. *J. Mol. Biol.* 216:1031–1044.

Kao, C.Y. 1986. Structure-activity relations of tetrodotoxin, saxitoxin and analogues. *Annu. NY Acad. Sci.* 479:52–67.

Lancelin, J.M., D. Kohda, S.I. Tate, Y. Yanagawa, T. Abe, M. Satake, and F. Inagaki. 1991. Tertiary structure of conotoxin GIIIA in aqueous solution. *Biochemistry.* 30:6908–6916.

Li, R.A., R.G. Tsushima, R.G. Kallen, and P.H. Backx. 1997. Pore residues critical for μ-CTX binding to rat skeletal muscle Na^+ channels revealed by cysteine mutagenesis. *Biophys. J.* 73:1874–1884.

Lipkind, G.M., and H.A. Fozzard. 1994. A structural model of the tetrodotoxin and saxitoxin binding site of the Na^+ channel. *Biophys. J.* 66:1–13.

Lu, Z., and R. MacKinnon. 1995. Probing a potassium channel pore with an engineered protonatable site. *Biochemistry.* 34: 13133–13138.

MacKinnon, R., and C. Miller. 1989. Mutant potassium channels with altered binding of charybdotoxin, a pore-blocking peptide inhibitor. *Science.* 254:1382–1385.

MacKinnon, R., L. Heginbotham, and T. Abramson. 1990. Mapping the receptor site for charybdotoxin, a pore-blocking potassium channel inhibitor. *Neuron.* 5:767–771.

MacKinnon, R., S.L. Cohen, A. Kuo, A. Lee, and B.T. Chait. 1998. Structural conservation in prokaryotic and eukaryotic potassium channels. *Science.* 280:106–109.

Moczydlowski, E., B.M. Olivera, W.R. Gray, and G.R. Strichartz. 1986. Discrimination of muscle and neuronal Na-channel subtypes by binding competition between [^{3}H]saxitoxin and μ-conotoxins. *Proc. Natl. Acad. Sci. USA.* 83:5321–5325.

Naranjo, D., and C. Miller. 1996. A strongly interacting pair of residues on the contact surface of charybdotoxin and a Shaker K^+ channel. *Neuron.* 16:123–130.

Olivera, B.M., J. Rivier, C. Clark, C.A. Ramilo, G.P. Corpuz, F.C. Abogadie, E.E. Mena, S.R. Woodward, D.R. Hillyard, and L.J. Cruz. 1990. Diversity of conus neuropeptides. *Science.* 249:257–263.

Ott, K.H., S. Becker, R.D. Gordon, and H. Ruterjans. 1991. Solution structure of μ-conotoxin GIIIA analysed by 2D-NMR and distance geometry calculations. *FEBS Lett.* 278:160–166.

Park, C.S., and C. Miller. 1992. Mapping function to structure in a channel-blocking peptide: electrostatic mutants of charybdotoxin. *Biochemistry.* 31:7749–7755.

Pérez-García, M.T., N. Chiamvimonvat, E. Marban, and G.F. Tomaselli. 1996. Structure of the sodium channel pore revealed by serial cysteine mutagenesis. *Proc. Natl. Acad. Sci. USA.* 93:300–304.

Pérez-García, M.T., N. Chiamvimonvat, R. Ranjan, J.R. Balser, G.F. Tomaselli, and E. Marban. 1997. Mechanisms of sodium/calcium selectivity in sodium channels probed by cysteine mutagenesis

and sulfhydryl modification. *Biophys. J.* 72:989–996.

Ranganathan, R., J.H. Lewis, and R. MacKinnon. 1996. Spatial localization of the K^+ channel selectivity filter by mutant cycle-based structure analysis. *Neuron.* 16:131–139.

Sato, K., Y. Ishida, K. Wakamatsu, R. Kato, H. Honda, Y. Ohizumi, H. Nakamura, M. Ohya, J.M. Lancelin, D. Kohda, and F. Inagaki. 1991. Active site of μ-conotoxin GIIIA, a peptide blocker of muscle sodium channels. *J. Biol. Chem.* 266:16989–16991.

Schild, L., and E. Moczydlowski. 1994. Permeation of Na^+ through open and Zn^{2+}-occupied conductance states of cardiac sodium channels modified by batrachotoxin: exploring ion-ion interactions in a multi-ion channel. *Biophys. J.* 66:654–666.

Schlief, T., R. Schonherr, K. Imoto, and S.H. Heinemann. 1996. Pore properties of rat brain II sodium channels mutated in the selectivity filter domain. *Eur. Biophys. J.* 25:75–91.

Schreiber, G., and A.R. Fersht. 1995. Energetics of protein-protein interactions: analysis of the Barnase-Barstar interface by single mutations and double mutant cycles. *J. Mol. Biol.* 248:478–486.

Serrano, L., A. Horovitz, B. Avron, M. Bycroft, and A.R. Fersht. 1990. Estimating the contribution of engineered surface electrostatic interactions to protein stability by using double-mutant cycles. *Biochemistry.* 29:9343–9352.

Stephan, M.M., J.F. Potts, and W.S. Agnew. 1994. The μI skeletal muscle sodium channel: mutation E403Q eliminates sensitivity to tetrodotoxin but not to μ-conotoxins GIIIA and GIIIB. *J. Membr. Biol.* 137:1–8.

Swartz, K.J., and R. MacKinnon. 1997. Mapping the receptor site for hanatoxin, a gating modifier of voltage-dependent K^+ channels. *Neuron.* 18:675–682.

Terlau, H., S.H. Heinemann, W. Stühmer, M. Pusch, F. Conti, K. Imoto, and S. Numa. 1991. Mapping the site of block by tetrodotoxin and saxitoxin of sodium channel-II. *FEBS Lett.* 293:93–96.

Todt, H., S.C. Dudley Jr., J.W. Kyle, R.J. French, and H.A. Fozzard. 1999. Ultra-slow inactivation in μ1 Na^+ channels is produced by a structural rearrangement of the outer vestibule. *Biophys. J.* 76: 1335–1345.

Tsushima, R.G., R.A. Li, and P.H. Backx. 1997. P-loop flexibility in Na^+ channel pores revealed by single- and double-cysteine replacements. *J. Gen. Physiol.* 110:59–72.

Wakamatsu, K., D. Kohda, H. Hatanaka, J.M. Lancelin, Y. Ishida, M. Oya, H. Nakamura, F. Inagaki, and K. Sato. 1992. Structure-activity relationships of μ-conotoxin GIIIA: structure determination of active and inactive sodium channel blocker peptides by NMR and simulated annealing calculations. *Biochemistry.* 31:12577–12584.

Wilkinson, A.J., A.R. Fersht, D.M. Blow, and G. Winter. 1983. Site-directed mutagenesis as a probe of enzyme structure and catalysis: tyrosyl-tRNA synthetase cysteine-35 to glycine-35 mutation. *Biochemistry.* 22:3581–3586.

Yamagishi, T., M. Janecki, E. Marban, and G.F. Tomaselli. 1997. Topology of the P segments in the sodium channel pore revealed by cysteine mutagenesis. *Biophys. J.* 73:195–204.